arXiv:1301.2972v1 [nlin.PS] 14 Jan 2013

Discrete flat-band solitons in the Kagome lattice

Rodrigo A. Vicencio[1] and Magnus Johansson[2]
[1]*Departamento de Física, MSI-Nucleus on Advanced Optics,*
and Center for Optics and Photonics (CEFOP),
Facultad de Ciencias, Universidad de Chile, Santiago, Chile and
[2]*Department of Physics, Chemistry and Biology,*
Linköping University, SE-581 83 Linköping, Sweden

We consider a model for a two-dimensional Kagome-lattice with defocusing nonlinearity, and show that families of localized discrete solitons may bifurcate from localized linear modes of the flat band with zero power threshold. Such fundamental nonlinear modes exist for arbitrarily strong nonlinearity, and correspond to unique configurations in the limit of zero inter-site coupling. We analyze their linear stability, and show that by choosing dynamical perturbations close to soft internal modes, a switching between solitons of different families may be obtained. In a window of small values of norm, a symmetry-broken localized state is found as the lowest-energy state.

PACS numbers: 42.65.Wi, 63.20.Pw, 63.20.Ry, 05.45.-a

INTRODUCTION

Discrete nonlinear systems have developed into an important area of research during the last years, where many theoretical and numerical predictions have been tested and proved experimentally [1–3]. In particular, nonlinear optics [2] and cold atoms [3] have shown to provide excellent implementations to restudy old and new theory, mainly coming from solid state physics. The fabrication of periodic and aperiodic structures, using different experimental techniques, has shown an enormous flexibility, where simple as well as very complicated lattice topologies can be obtained in a simple and controlled way in different dimensions.

There are general theories describing the bifurcation of families of nonlinear localized modes ("gap solitons") from linear band edges when a weak nonlinearity is added to some spatially periodic Hamiltonian system (see, e.g., Ref. [4] and references therein). In generic situations, when the band edge is a non-degenerate local minimum or maximum with non-zero group-velocity dispersion, perturbation theory for weak nonlinearity yields a nonlinear Schrödinger (NLS) equation for the slowly varying amplitude of solutions close to the band edge. In the most common case of an effective cubic (Kerr) nonlinearity, one may then conclude from the properties of the corresponding NLS solitons that in one dimension (1D), localized gap solitons bifurcate from the linear band edge with zero power (norm), while in two dimensions (2D) the bifurcating solution appears at a non-zero power, resulting in a generic *excitation threshold* for gap solitons in two (and also higher) dimensions [5]. In both cases, the soliton envelope decays exponentially with a localization length that diverges in the linear limit.

However, there are some particularly interesting classes of lattices where the above mentioned conditions are not fulfilled. Probably the most well-known example is the 2D Kagome lattice, where one of the tight-binding bands (the lowest-energy one with the sign-conventions used below) is completely flat, and in addition it touches the extremum of the second band at one point so that also the latter becomes degenerate (see, e.g., [6] and references therein). It is therefore an open question, which we here aim at resolving, if and how solitons may bifurcate also from such flat-band linear modes.

The study of Kagome lattices has a long history, in particular as a prototype system for geometrically frustrated magnetism (see, e.g., [7]). Recently, successful syntheses of artificial Kagome lattices have been reported in several contexts; e.g., nondiffracting Kagome lattice for light beams were obtained in [8], photon-based litography was used to fabricate Kagome lattice structures in [9], in [10] a Kagome optical lattice was realized for trapping ultracold atoms, and in [11] a metallic Kagome lattice was fabricated and a flat plasmonic band observed. Thus, the technology to experimentally observe physical phenomena arising from the presence of a flat dispersion band in a nonlinear lattice appears to be within reach.

Effects of including interactions in Hubbard-type models on Kagome lattices have been discussed for fermionic [12] as well as bosonic [13] systems, and in both cases shown to result in an effective gap opening between the lowest-energy flat band and the second band at a certain filling factor for sufficiently strong interaction. These gap openings were related to a breaking of the translational symmetry of the ground states of the non-interacting lattices.

Concerning localized structures in classical nonlinear Kagome lattices with defocusing nonlinearity, a number of such structures were described in [14]. However, these authors focused on complex structures such as vortices and their properties in the limit of strong nonlinearity, and did not at all discuss the fundamental modes and their connections to the linear flat-band modes (in fact, Ref. [14] does not even mention the existence of a flat linear band). More recent works discuss defect solitons in Kagome optical lattices with saturable nonlinearity [15] and localization of light in Kagome nanoribbons [16]; however, both these works considered exclusively the case of focusing nonlinearity with solitons bifurcating from the edge of the upper band, which is non-degenerate and therefore these solitons follow the standard NLS phenomenology in 2D with excitation threshold [1, 5].

We here study a Kagome lattice with cubic nonlinearity by considering the following DNLS-like equation:

$$i\frac{\partial u_{\vec{n}}}{\partial z}+\sum_{\vec{m}}V_{\vec{n},\vec{m}}u_{\vec{m}}+\gamma|u_{\vec{n}}|^2u_{\vec{n}}=0\ , \tag{1}$$

where z corresponds to the normalized dynamical coordinate, γ to an effective nonlinear cubic parameter, and $u_{\vec{n}}$ represents the field amplitude at site $\vec{n}$ in a 2D Kagome lattice [see Fig. 1(a)]. The coupling function $\sum_{\vec{m}}V_{\vec{n},\vec{m}}u_{\vec{m}}$ defines the linear interactions between $u_{\vec{n}}$ and its nearest neighbors. Model (1) possesses two conserved quantities, the norm (power) defined as $P=\sum_{\vec{n}}|u_{\vec{n}}|^2$, and the Hamiltonian (energy) defined as $H=-\sum_{\vec{n}}\left\{\sum_{\vec{m}}V_{\vec{n},\vec{m}}(u_{\vec{m}}u_{\vec{n}}^*+u_{\vec{m}}^*u_{\vec{n}})+(\gamma/2)|u_{\vec{n}}|^4\right\}$. Unless otherwise stated, the defocusing nonlinear lattice is obtained by fixing $\gamma=-1$, and $V_{\vec{n},\vec{m}}=1$ for nearest neighbors and zero otherwise.

Linear solutions ($\gamma=0$) are obtained by solving model (1) with a stationary ansatz of the form $u_{\vec{n}}(z)=u_{\vec{n}}\exp(i\lambda z)$. To obtain the linear spectrum (cf., e.g., [6, 11–13]), we first consider an infinite system and three fundamental sites belonging to a unit cell of the lattice [triangle in Fig. 1(a)]. We construct the corresponding 2D $\vec{k}$-vectors and obtain three different linear bands:

$$\lambda(k_x,k_y)=-2,\ 1\pm\sqrt{1+8f(k_x,k_y)}\ , \tag{2}$$

where $f(k_x,k_y)\equiv1+2\cos^4(k_x/2)-3\cos^2(k_x/2)-\cos^2(\sqrt{3}k_y/2)+2\cos^2(k_x/2)\cos^2(\sqrt{3}k_y/2)$. Fig. 1(b) shows a 3D plot of the band structure in the first Brillouin zone. The upper and lower bands are "connected" at $\lambda=1$ by six Dirac points located at the vertices of the hexagon forming the Brillouin zone [$f(k_x,k_y)=-1/8$]. A sketch of the fundamental modes associated to the top of the upper band and to the bottom of the lower band are shown in Figs. 1(c) and (d), for a finite-size lattice with rigid boundary conditions. The largest eigenvalue mode has a typical structure resembling the fundamental mode of any 2D system, where all sites oscillate in phase with a decaying amplitude due to the open boundary conditions. The smallest eigenvalue mode of the lower band possesses a structure reminiscent of a staggered mode; however, due to the particular geometry of the Kagome lattice it is not possible to construct a fully staggered mode, but a "frustrated" state like the one shown in Fig. 1(d). Note that, in contrast to the case with periodic boundary conditions, this eigenvalue is slightly larger than -2 for rigid boundary conditions, and therefore this band does not touch the flat band at -2 [6].

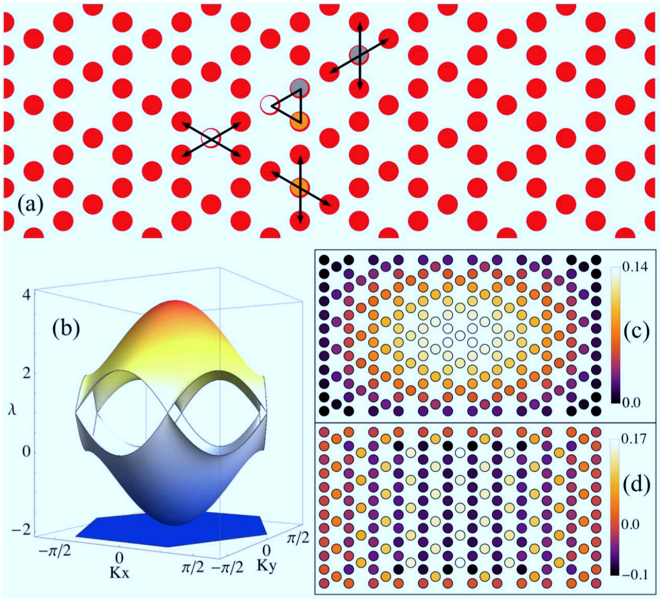

Figure 1: (Color Online) (a) Kagome lattice structure with a unit cell of three fundamental sites, including their interactions. (b) Band structure. Linear modes profiles at $\lambda=3.91$ (c), and $\lambda=-1.98$ (d), for a lattice of 205 sites with rigid boundary conditions.

The third degenerated-flat band, located exactly at $\lambda=-2$, possesses as many states as the number of closed rings in the lattice (being infinite for an infinite system) [6]. These states – called "6-peaks" or "ring" solutions – have 6 peaks with equal amplitude but alternating sign (phase), with a strictly zero background [see Fig. 2(a)-inset]. These ring (hexagon) modes constitute "building blocks" for a Kagome lattice. Any linear combination of them will generate an exact linear stationary solution of the system.

Therefore, a fundamental question concerning nonlinear solutions bifurcating from some specific linear combination of these modes arises. Let us first compute this ring stationary solution in the nonlinear regime. It is simple to show, that each ring mode of the flat band can be exactly continued into a nonlinear mode with *exactly the same configuration*, only with a frequency shift; thus these solutions are "exact discrete compactons" [17]. For any nonlinear ring mode, the frequency shift and power are related as $P=6(\lambda+2)/\gamma$.

For a defocusing nonlinearity ($\gamma<0$), all fundamental nonlinear solutions bifurcate at $\lambda=-2$ ($P=0$) from some linear combination of these ring modes. Generally in discrete nonlinear systems, a "one-peak solution" is often identified as a family of solutions approaching a single-site localized state in the strong-nonlinearity/weak coupling ("anticontinuous") limit, and typically corresponds to the geometrically simplest fundamental nonlinear mode bifurcating from the linear modes at the band borders [5]. For a Kagome lattice, a mode with these properties can be constructed by combining two neighboring rings, having one common central site. In the linear limit, this site will get twice the amplitude of the other ring sites. For non-zero nonlinearity, this - compact - solution will no longer be exact; instead, it will develop into a discrete soliton state with exponentially decaying tails, which continues smoothly to a single-site solution at the anticontinuous limit (larger norms). Therefore, the effective size of this solution will drastically decrease being, for some value of the norm, smaller than the ring solution. Therefore, we may expect an exchange of fundamental properties between the ring and the one-peak solutions if compared at a given norm (compare, e.g., similar features for saturable systems, where multiple changes on the effective size of fundamental solutions produce changes in their stability properties [18–20]).

We construct these two fundamental families (the one-peak and six-peaks solutions) and show the results in Fig. 2. The $P-\lambda$ diagram [Fig. 2(a)] shows how these modes bifurcate from the flat band at $P=0$, i.e., *without excitation threshold*. Moreover, these solutions are very localized for lower values of the norm being, therefore, very unusual 2D discrete solitons originating in the particular topology of this lattice and its fundamental building blocks. [In fact, Fig. 2(a) is more similar to what is obtained for 1D cubic lattices]. For larger norms, these two solutions strongly deviate, the norm content of the ring solution being much larger.

In Fig. 2(b) we show a $\Delta H-P$ diagram, for $\Delta H \equiv H_i - H_{ring}$ (i represents any solution). For smaller values of the norm, we see how the ring solution ($\Delta H = 0$) corresponds to the ground state bifurcating from the linear band at zero norm. Then, we observe a crossing point at $P \approx 0.43$, between the one- and the six-peaks solutions, that indicates an exchange of stability properties. To calculate the linear stability of these solutions, a standard procedure is implemented [21]: we obtain the linear eigenvalue spectrum $\{\omega^2 \equiv g\}$ and compute the largest $G \equiv \sqrt{[|g|-g]/2}$. A stable solution corresponds to $G=0$ while $G \neq 0$ to an unstable one. The $G-P$ diagram in Fig. 2(c) confirms that for small values of the norm, the six-peaks solution is stable (ground state) while the one-peak mode is unstable. For $0.32 \lesssim P \lesssim 0.51$, we observe an instability inversion regime with a region of bi-instability and, therefore, that none of the fundamental solutions correspond to minima in a Hamiltonian representation. Thus, in this regime a new stationary solution – corresponding to a minimum in-between them – should appear, connecting them in parameter space. For larger power, the one-peak solution is always stable (minimum) while the ring mode is unstable.

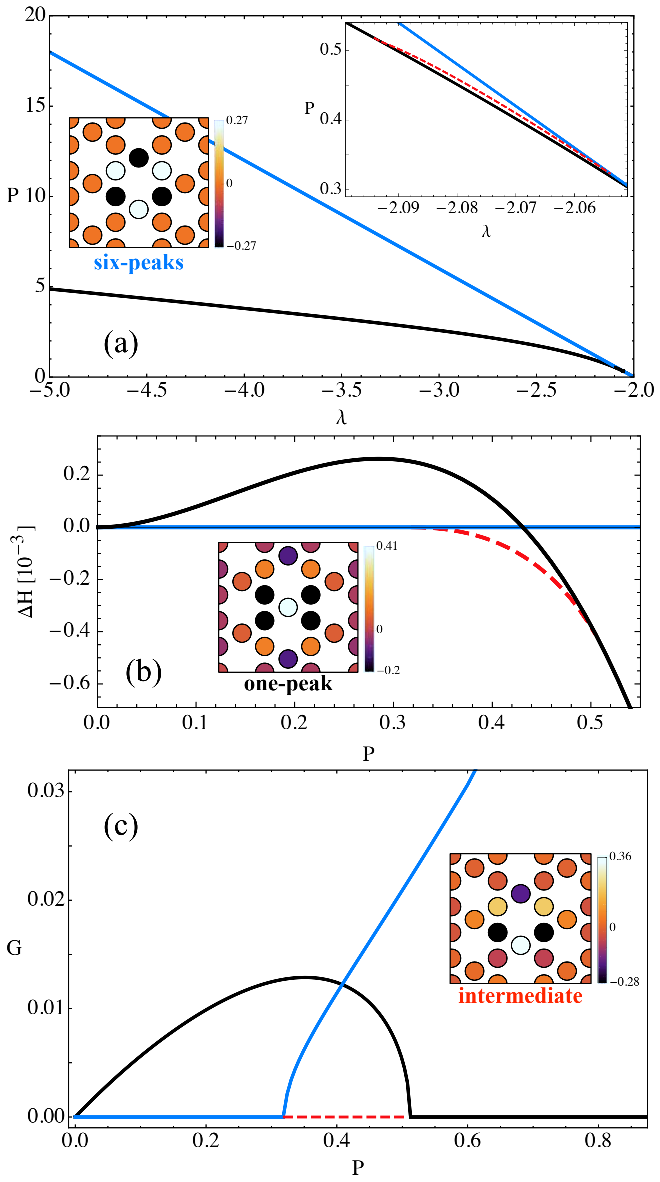

Figure 2: (Color Online) (a) P vs λ, (b) ΔH vs P, and (c) G vs P diagrams. The one-peak, ring, and intermediate solutions are shown with black, blue and red-dashed lines, respectively. Insets show profiles of the stationary modes for $P=0.43$.

The solution corresponding to a minimum in the bi-unstable region is known as "Intermediate Solution" (IS) and constitutes a *symmetry-broken stationary solution* appearing when the stability properties of fundamental solutions are exchanged [18–20, 22, 23]. In the present case we find a stable IS [23, 24] in-between two unstable fundamental modes (in other contexts, the opposite is also possible [18, 19, 22, 23]). In Fig. 2 (red-dashed line) we show the appearance of the IS connecting the two fundamental modes. In the stability diagram [Fig. 2(c)] we observe how the IS is stable in the region where the two fundamental modes are unstable simultaneously. Fig. 2(b) shows the emergence of the IS connecting the ring solution with the one-peak mode. In its existence

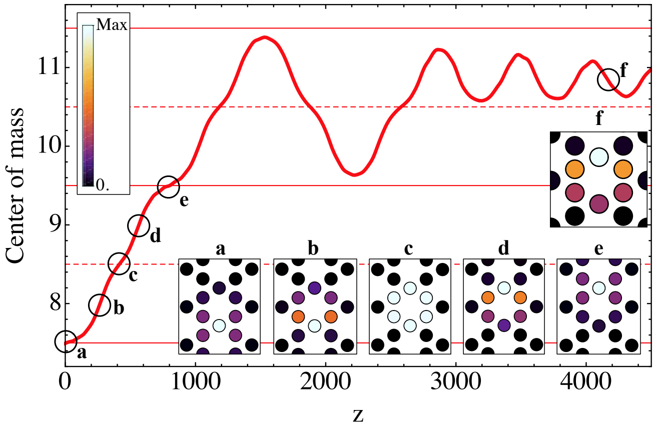

Figure 3: (Color Online) Vertical center of mass evolution of an unstable one-peak solution for $P = 0.4655$, $k_x = 0$, $k_y = 0.009$. Insets: zoom of different profiles $|u_{\vec{n}}(z)|^2$. Horizontal full (dashed) lines represent the one-(six-)peaks solutions.

region, the IS possesses the smaller Hamiltonian value and constitutes an effective *ground-state* of the system.

As we will exemplify by exploring the dynamics of an unstable one-peak solution and observing its evolution, symmetry-broken ground states may appear spontaneously. By inspecting the unstable internal mode of the one-peak solution [25], we notice that it essentially corresponds to a deformation in the vertical direction, which is similar to the introduction of a phase gradient in the profile: $u_{\vec{n}} \exp(i\vec{k} \cdot \vec{n})$, with $\vec{k}$ a "kick" vector. Fig. 3 shows the result of applying a small kick in the vertical direction, showing a slow and smooth movement of a low-norm and very localized solution. We see how the effective Hamiltonian (Peierls-Nabarro) potential is traced and the velocity of the center of mass changes accordingly (cf., e.g., [18, 19]). The regions with largest velocity correspond to minima of the effective potential, which in this case correspond to the intermediate stationary solutions with profiles possessing a geometry in-between the one and the six-peaks solutions. The mobility of this solution generates some radiation that decreases the power of the moving profile. Although the solution starts in a norm region where the one-peak solution has a lower H-value than the six-peaks [see Fig. 2(b)], it rapidly moves to a region below the crossing point. Therefore, the solution moves faster when passing through a Ring solution than when passing through a one-peak mode. In fact, for the small kick used, the solution is able to jump coherently one complete site in the vertical direction and then it cannot continue traveling further due to radiation losses (bounce at $z \sim 1500$). Then, it oscillates passing through ring modes and intermediate solutions, without being able to overcome the one-peak barrier (horizontal full lines in Fig. 3). Finally, it gets trapped oscillating around the symmetry-broken ground state.

The possibility of moving a very localized solution across the lattice is certainly an important issue in different physical contexts. Typical 2D nonlinear cubic lattices do not allow mobility of highly localized excitations [26], which are thought to be the key entities for controlling the propagation of information – in the form of waves – in periodical media. By choosing different phase gradients, we were able to move one- and six-peaks profiles across the whole lattice. For example, by giving a vertical kick of $k_y = 0.25$ to a one-peak mode of $P = 0.502$, we observe a translation of six unit cells in the vertical direction (the excitation stopped because of borders and radiation effects). While moving, solutions generate some radiation and the dynamics is not as soft as the one shown in Fig. 3. Nevertheless, coherent mobility of highly localized solutions is allowed due to the Kagome topology.

In conclusion, we showed, using the Kagome lattice as example, how nonlinear localized modes can bifurcate from a highly degenerate, dispersion-less linear band without excitation threshold. We identified two types of fundamental modes, which were shown to exchange their stability and therefore could be switched into each other through a symmetry-broken intermediate state, which constitutes the ground state around the exchange region. Since this scenario appears already for a weak (Kerr) nonlinearity, and involves states which are strongly localized due to the flatness of the linear band, it could be of large relevance for practical applications. While for simple cubic regular DNLS lattices symmetry-broken ground states do not appear and stability properties are never exchanged between fundamental modes, the topology of the Kagome lattice allows the appearance of new solutions that can be crucial to improve the dynamical properties of these nonlinear systems. This opens new possibilities for controlling the propagation of waves in such systems.

Authors thanks U. Naether for useful discussions. M.J. thanks the Nonlinear Optics Group, Universidad de Chile, for kind hospitality, and acknowledges support from the Swedish Research Council. This work was supported in part by FONDECYT grant 1110142, CONICYT fellowships, Programa ICM P10-030-F, and Programa de Financiamiento Basal de CONICYT (FB0824/2008).

[1] S. Flach and A.V. Gorbach, Phys. Rep. **467**, 1 (2008).
[2] F. Lederer, G.I. Stegeman, D.N. Christodoulides, G. Assanto, M. Segev, and Y. Silberberg, Phys. Rep. **463**, 1 (2008).
[3] O. Morsch and M. Oberthaler, Rev. Mod. Phys. **78**, 179 (2006).
[4] T. Dohnal and D. Pelinovsky, Phys. Rev. E **85**, 026605 (2012).
[5] S. Flach, K. Kladko, and R.S. MacKay, Phys. Rev. Lett.

78, 1207 (1997).

[6] D.L. Bergman, C. Wu, and L. Balents, Phys. Rev. B **78**, 125104 (2008).

[7] J.L. Atwood, Nature Materials **1**, 91 (2002).

[8] M. Boguslawski, P. Rose, and C. Denz, Appl. Phys. Lett. **98**, 061111 (2011).

[9] L. Wang *et al.*, Appl. Phys. Lett. **101**, 093104 (2012).

[10] G.-B. Jo *et al.*, Phys. Rev. Lett. **108**, 045305 (2012).

[11] Y. Nakata, T. Okada, T. Nakanishi, and M. Kitano, Phys. Rev. B **85**, 205128 (2012).

[12] S. Nishimoto, M. Nakamura, A. O'Brien, and P. Fulde, Phys. Rev. Lett. **104**, 196401 (2010).

[13] S.D. Huber and E. Altman, Phys. Rev. B **82**, 184502 (2010).

[14] K.J.H. Law, A. Saxena, P.G. Kevrekidis, and A.R. Bishop, Phys. Rev. A **79**, 053818 (2009).

[15] X. Zhu, H. Wang, and L.X. Zheng, Optics Express **18**, 20786 (2010).

[16] M.I. Molina, Phys. Lett. A **376**, 3458 (2012).

[17] P.G. Kevrekidis and V.V. Konotop, Phys. Rev. E **65**, 066614 (2002); P.G. Kevrekidis, V.V. Konotop, A.R. Bishop, and S. Takeno, J. Phys. A **35**, L641 (2002).

[18] R.A. Vicencio and M. Johansson, Phys. Rev. E **73**, 046602 (2006).

[19] U. Naether, R.A. Vicencio, and M. Johansson, Phys. Rev. E **83**, 036601 (2011).

[20] U. Naether, R.A. Vicencio, and M. Stepić, Opt. Lett. **36**, 1467 (2011).

[21] A. Khare, K.Ø. Rasmussen, M.R. Samuelsen, and A. Saxena, J. Phys. A **38**, 807 (2005).

[22] T. Cretegny, Ph.D. thesis (in French), École Normale Supérieure de Lyon, 1998; S. Aubry, Physica D **216**, 1 (2006).

[23] M. Öster, M. Johansson, and A. Eriksson, Phys. Rev. E **67**, 056606 (2003).

[24] S. Rojas-Rojas, R.A. Vicencio, M.I. Molina, and F.Kh. Abdullaev, Phys. Rev. A **84**, 033621 (2011).

[25] See Supplemental Material for illustration of the linear spectra and eigenmodes of the fundamental solutions in the low-power regime.

[26] E. Arévalo, Phys. Rev. Lett. **102**, 224102 (2009).

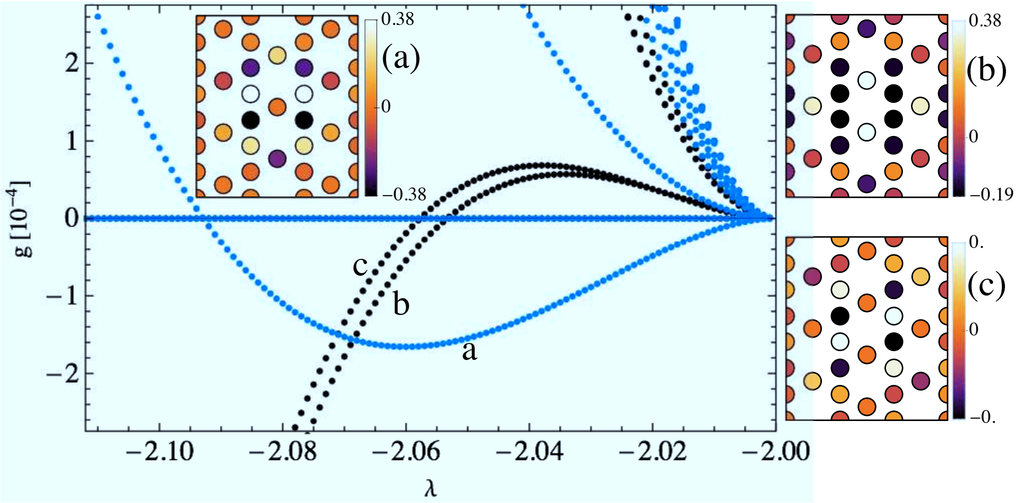

Figure 4: The main figure shows the linear spectra g versus λ of the one-site (blue dots) and one-ring (black dots) solutions in the regime of weak nonlinearity. Insets (a)-(c) show the profiles of the indicated linear modes. It is seen how the flat band spreads out due to the spatial symmetry breaking caused by the particular nonlinear localized fundamental mode excited, and how isolated localized linear eigenmodes bifurcate from this band. For the one-site solution there is one such mode which is unstable, while for the one-ring mode there are two stable (soft) internal modes close to the linear limit. One of these modes then becomes unstable in the bifurcation where the symmetry-broken intermediate solution is born (the second mode also becomes unstable slightly afterwards). Seen from the linear limit, one can see how a gap opens around zero, which is a classical counterpart to the gap openings due to interactions in quantum Hubbard models [12, 13].